Mon. Not. R. Astron. Soc. **263**, 335–342 (1993)

# The nebular remnant and quiescent spectrum of Nova GK Persei

G. C. Anupama[1,2] and T. P. Prabhu[1]

[1] *Indian Institute of Astrophysics, Bangalore 560034, India*
[2] *Inter-University Centre for Astronomy and Astrophysics, Post Bag 4, Ganeshkhind, Pune 411007, India*

Accepted 1993 January 19. Received 1992 November 5; in original form 1992 April 10

**ABSTRACT**

CCD images of the nebular shell of the old nova GK Per in [N II] and [O III] emission lines, and also the quiescent spectrum in the optical region, are presented. Proper motion measurements of the knots in [N II] over the baseline 1984–90 give a mean expansion rate of $0.31 \pm 0.07$ arcsec yr$^{-1}$. This value agrees with models of the expansion of the ejecta into the ambient circumstellar medium. A correction for projection effects indicates that the ratio of the mass of the shell to the density of the circumstellar medium is a factor of 2–3 higher than estimated previously. The optical spectrum is decomposed into those of the secondary and the accretion disc. The estimate of $M_V = +4.9$ for the accretion disc implies a mass transfer rate of $3.5 \times 10^{-9}$ $M_\odot$ yr$^{-1}$ in the steady state. The H and He emission-line fluxes are used to infer that (i) the line-emitting region has a high density, (ii) the He/H abundance is near-solar, and (iii) the ionizing source has a Zanstra temperature of $1.3 \times 10^5$ K and an effective radius of 0.01 $R_\odot$, which are consistent with its being a white dwarf.

**Key words:** accretion, accretion discs – circumstellar matter – stars: individual: GK Per – novae, cataclysmic variables – white dwarfs.

## 1 INTRODUCTION

GK Persei (Nova Persei 1901) was the first bright nova of the twentieth century, and was subjected to very detailed spectroscopy and photographic photometry (Payne-Gaposchkin 1957). In contrast with most old novae, GK Per exhibits dwarf-nova-like outbursts of ~ 3 mag, the latest of which was in 1992 (Hurst 1989) (see Vogt 1989 for a list of other classical novae exhibiting dwarf nova activity during quiescence). These outbursts are thought to start at the inner edge of the accretion disc, where an unstable region can occasionally form as a result of modulation of the mass transfer rate from the secondary (Cannizzo & Kenyon 1986; Bianchini et al. 1986; Kim, Wheeler & Mineshige 1992). Of the known classical novae, GK Per has by far the longest orbital period (1.997 d) and, unlike other novae, has an evolved secondary of type K0IV (Crampton, Cowley & Fisher 1986). The eccentricity of the orbit is uncertain. Bianchini, Hamzaoglu & Sabbadin (1981) suggested a highly eccentric orbit, $e = 0.39$, whereas Crampton et al. determined an essentially circular orbit. The mass of the white dwarf primary is estimated to be 0.9 $M_\odot$, and that of the secondary is thought to be 0.25 $M_\odot$ (Crampton et al. 1986). The orbital inclination is uncertain, but the absence of obvious eclipses indicates that it cannot be very high: $i \leq 73°$ (Crampton et al. 1986), or $i = 66°$ (Bianchini & Sabbadin 1983). A long-term solar-type activity of the secondary has been detected with a periodicity of ~ 7 yr (Bianchini 1990). GK Per was one of the first cataclysmic variables to be identified with an X-ray source. Observations with *EXOSAT* revealed very strong pulsed radiation with a period of 351 s, establishing GK Per as a member of the DQ Her class of objects (Watson, King & Osborne 1985; Norton, Watson & King 1988). This periodicity, which is attributed to the spin of the magnetized white dwarf, has also been detected in the optical, and there is some evidence for the spin-up of the white dwarf (Patterson 1991, and references therein).

The optical spectrum of GK Per contains strong emission lines of H, He I and He II from the accretion disc around the primary (Gallagher & Oinas 1974). Ca II 3934 Å is weakly present in emission. Absorption features due to the secondary are also present: Na I D and Ca I 4227 Å, and lines of Fe I, Cr I, Ti I and Mg I (Kraft 1964; Gallagher & Oinas 1974). Based on the Ca I 4227-Å equivalent width, and the strength of other absorption lines, Gallagher & Oinas assigned a type K2V–IV to the secondary, in agreement with Kraft (1964). The secondary is estimated to contribute about 33 per cent of the total light in the blue.

A month after the 1901 outburst, expanding nebulosities were seen in the vicinity of the nova (e.g. Ritchey 1901;

Perrine 1902). This first recorded 'light echo' was explained by Couderc (1939) in terms of reflection from dust grains lying in a plane crossing the line of sight to the nova. The fact that no other nova (with the exception of V732 Sgr 1936: Swope 1940) has shown such a phenomenon led Schaefer (1988) to suggest that the grain density in the light-echo region of GK Per is up to $10^4$ times that in the general interstellar medium. The expanding ejecta from the 1901 outburst were first discovered by Barnard in 1916 (see Curtis 1919) and photographed by Pease (1947), and have been intermittently followed ever since. The asymmetry and longevity of this remnant are quite unusual and unique among novae. The evolution of the optical nebulosity over several decades indicates that the expanding ejecta are interacting with the ambient medium (Seaquist et al. 1989, hereinafter S89). Duerbeck (1987) has measured the resultant deceleration of the south-western bar where the interaction is most prominent. S89 have fitted the observed radii at different epochs with theoretical models of expansion in the ambient medium.

The remnant of GK Per and its environs have been studied in detail by Bode et al. (1987) and S89. Extended emission associated with GK Per has been detected in the far-infrared: the 60- and 100-μm *IRAS* images show the presence of an elongated structure running roughly from north-west to south-east through the position of the nova. This extension, which is about 40 arcmin in size, is coincident with the H I emission, and is double-peaked, the novae residing on a saddle point between the peaks. There is no significant change in temperature across the IR extension. It has been suggested that the IR and H I emission arise from a torus of material surrounding GK Per, viewed almost edge-on. The distribution of the CO emission (Hessman 1989) also coincides with the IR and H I emission. The torus is probably the result of planetary nebula ejection from the central binary during its common-envelope phase of evolution, and the estimated age of the planetary nebula is $3 \times 10^4$ to $1.3 \times 10^5$ yr.

The remnant of GK Per has been imaged in broad-bands as well as in emission lines ([N II], [O III], [O II]), both photographically and, in recent times, using CCDs. Optical images of the expanding ejecta obtained over several decades show that the shell is highly asymmetric and has evolved into a series of knots. The bulk of the emission arises in the south-western quadrant. [O III] images, however, show little emission in this region. Recent images of the shell (Seitter & Duerbeck 1987; S89) suggest a box-shaped structure, with evident flattening to the south-west and north-east. This flattening is due to the deceleration of the ejecta on interaction with the ambient medium. In a 4.86-GHz radio image obtained by S89, the ridge of maximum radio brightness coincides with the flattened south-western portion of the optical shell, indicating interaction between the nova ejecta and the ambient gas. The radio emission is non-thermal, synchrotron radiation being the predominant emission mechanism. Based on radio observations, Reynolds & Chevalier (1984) and S89 concluded that in many respects the remnant of GK Per behaves like a supernova remnant. The angle subtended at the nova by the south-western interaction zone has remained constant over several decades, suggesting that the interacting circumstellar gas is confined to a polar cone with an opening angle of 90° and an axis perpendicular to the axis of the bipolar nebula (S89).

## 2 THE NEBULAR REMNANT

### 2.1 Observations

Optical CCD images of the nebular shell around GK Per were obtained at Vainu Bappu Observatory (VBO), Kavalur using the 1-m reflector and Photometrics CCD system, in the H$\alpha$ + [N II] and [O III] emission lines. A Thomson-CSF TH 7882 CDA CCD chip coated for UV response enhancement was used. At the *f*/13 Cassegrain focus, the image scale corresponds to 0.36 arcsec per pixel, with a total field of view of $2.3 \times 3.4$ arcmin$^2$. The [O III] images (50-Å bandpass, $2 \times 45$ min) were obtained on 1989 February 5, and the H$\alpha$ + [N II] images (160-Å bandpass) on 1988 December 8 (30 min), 1990 January 17 ($2 \times 30$ min) and 1990 February 20 (30 min).

All images were individually debiased and flat-field-corrected. Flat-field images were obtained from twilight sky exposures. The processed images were aligned using a shift + rotation transformation. The aligned H$\alpha$ + [N II] images from 1990 January 17 and February 20 were averaged. Likewise, a mean [O III] image was obtained, which was aligned with respect to the mean H$\alpha$ + [N II] image. It was found that the [O III] filter produced a 'ghost image' of the central star due to a slight inclination of the filter with respect to the optical axis of the incoming beam. This 'ghost' was detected, at 2 per cent of the original intensity level, for the central star only, while other stars in the field that were fainter than GK Per did not show it. The faint nebulosity around GK Per is hence unaffected. Since the 'ghost' had a star-like appearance, a Lorentzian profile was computed and the model fit subtracted out to remove it.

All reductions were carried out using the Starlink EDRS package at the VAX 11/780 installation at VBO, with locally developed routines for interaction with the COMTAL image processing unit.

### 2.2 Description of the shell

Fig. 1 shows the contour diagram of the mean H$\alpha$ + [N II] image, and Fig. 2 shows the contour diagram of the mean [O III] image. The H$\alpha$ + [N II] image predominantly contains [N II] emission, which is at least 20 times as strong as H$\alpha$ (S89). Though the shell appears asymmetric at first sight, some symmetries become apparent when emissions in both the lines are examined. An enhancement of [O III] emission over [N II] is seen around position angles 130° and 300°. This is also apparent in fig. 3 of Seitter & Duerbeck (1987), which is a positive–negative composite of the two lines. These position angles coincide with the extended IR torus and H I emission from the old planetary nebula. The [N II] and radio emissions are enhanced in the directions perpendicular to the torus. S89 argued that the suppression of [O III] in these directions can be explained by a model involving interaction of the nova ejecta with the ambient medium due to a previous slow polar outflow. We will henceforth identify the direction of this outflow as 'polar' and the direction of the extended emission as 'equatorial'. The images published by S89 show that [O II] is strong in both equatorial and polar directions. We thus have strong [O II] and [O III] and moderate [N II] in the equatorial direction, and strong [N II], [O II] with weak [O III] in the polar direction. It is significant that the equatorial and polar directions suggested by S89, based on extended emission, agree with the emission struc-

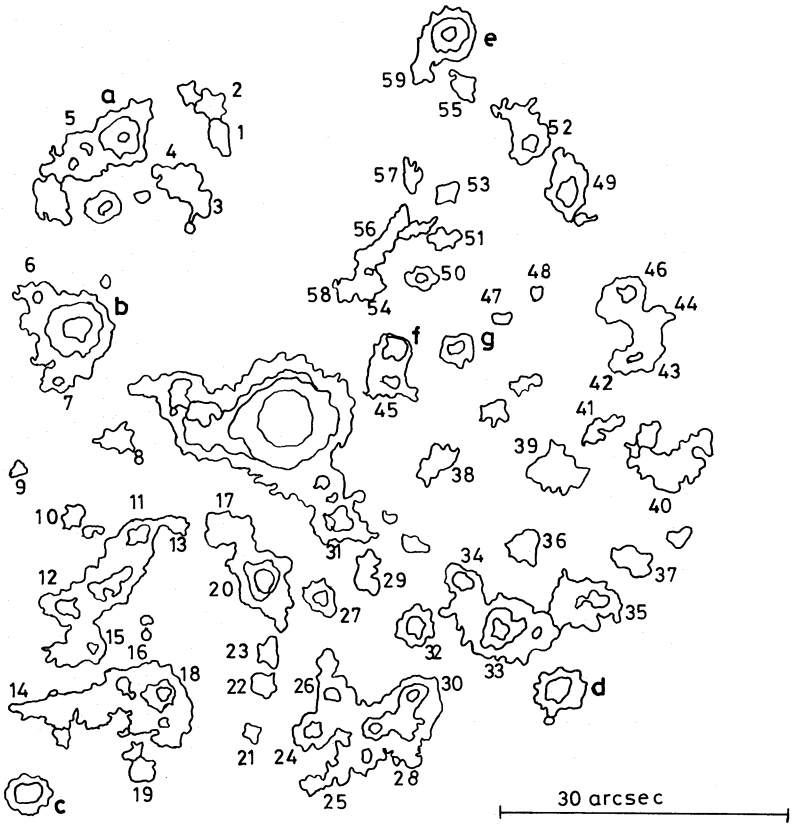


**Figure 1.** Contour diagram of the H$\alpha$+[N II] image of the GK Per shell. Knots for which proper motion has been measured are marked. The stars in the field are labelled a–g. North is at the top and east to the left.

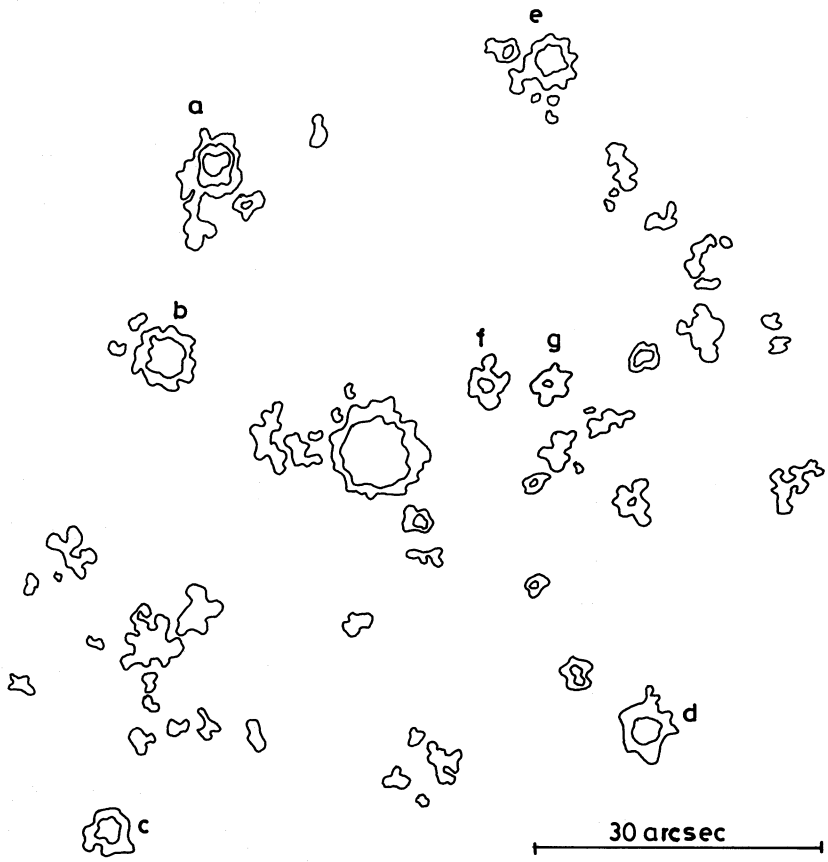


**Figure 2.** Contour diagram of the [O III] image of the GK Per shell. North is at the top and east to the left.

ture of the nebula. There appears to be a basic parameter (possibly angular momentum) which has determined the geometry of ejection of both the planetary nebula and the nova shell.

The enhancement of [O II] as well as [O III] emission in the equatorial ring suggests an enhancement of oxygen over nitrogen in this region. Differences in the spatial distribution of O and N in the polar and equatorial regions of nova shells have been suggested by Seitter & Duerbeck (1987).

### 2.3 Kinematics of the shell

We have measured the proper motions ($\mu$ in arcsec yr$^{-1}$) of individual knots in the [N II] image (Fig. 1), by comparing our image (epoch 1990.10) with the 1984 August image of S89 (epoch 1984.63). The 1984 image obtained with the Calar Alto 2.2-m reflector has an image scale which closely matches our image. The measurements were made using the NOAO subpackage of IRAF at the Inter-University Centre for Astronomy and Astrophysics (IUCAA), Pune. Only the knots for which reasonable and mutually agreeing Gaussian fits were possible were accepted for the final analysis. Our 1988 image was not used, since the baseline would have been too small. The two images were transformed to a common scale using a rotation and magnification transformation with the coordinate system referred to the centre of the stellar image of GK Per, using the field stars a–g (Fig. 1) as reference. The accuracy of the transformation as reflected in the proper motion data can be judged from the mean derived proper motion for these stars: $0.002 \pm 0.035$ arcsec yr$^{-1}$ in the radial direction and $0.005 \pm 0.018$ arcsec yr$^{-1}$ in the transverse direction. The derived radial proper motions for 20 knots are listed in Table 1. The mean proper motion is $0.31 \pm 0.07$ arcsec yr$^{-1}$. The mean transverse proper motion for the knots is $-0.02 \pm 0.04$ arcsec yr$^{-1}$, which is indicative of the expected errors of measurement.

The mean proper motion of the knots in the south-western interaction zone is $\mu = 0.33 \pm 0.06$ arcsec yr$^{-1}$. On the other hand, an extrapolation of the constant-deceleration model of Duerbeck (1987) at the mean epoch of 1987.37 ($t - t_0 = 86.23$ yr) yields a value of 0.17 arcsec yr$^{-1}$, whereas the detailed momentum-conserving and energy-conserving expansion models of S89 yield values of 0.33 and 0.35 arcsec yr$^{-1}$, respectively. It is thus seen that the measured proper motions agree better with S89 than with Duerbeck. This is to be expected, since a constant-deceleration model is valid only for time-scales much smaller than the characteristic deceleration time-scales ('half-life' = 58 yr for GK Per: Duerbeck 1987).

**Table 1.** Radii, position angles and proper motions of bright [N II] knots in the shell of GK Per.

| # | $r$ arcsec | $\theta$ deg | $\mu$ arcsec yr$^{-1}$ | $\mu/r$ yr$^{-1}$ |
|---|---|---|---|---|
| 7 | 25.0 | 89.0 | 0.22 | 0.0089 |
| 11 | 20.4 | 138.0 | 0.23 | 0.0111 |
| 15 | 33.1 | 148.3 | 0.36 | 0.0108 |
| 18 | 33.2 | 164.0 | 0.38 | 0.0113 |
| 19 | 42.3 | 166.0 | 0.37 | 0.0088 |
| 24 | 34.4 | 192.7 | 0.37 | 0.0107 |
| 28 | 35.5 | 209.1 | 0.38 | 0.0106 |
| 32 | 26.3 | 219.6 | 0.29 | 0.0110 |
| 33 | 31.6 | 234.3 | 0.32 | 0.0100 |
| 34 | 25.6 | 235.7 | 0.21 | 0.0083 |
| 35 | 37.3 | 248.0 | 0.36 | 0.0095 |
| 36 | 28.8 | 250.0 | 0.33 | 0.0115 |
| 37 | 39.6 | 256.9 | 0.43 | 0.0108 |
| 39 | 28.3 | 268.3 | 0.26 | 0.0091 |
| 40 | 41.3 | 272.0 | 0.33 | 0.0081 |
| 46 | 39.2 | 300.6 | 0.32 | 0.0080 |
| 47 | 25.9 | 304.9 | 0.27 | 0.0102 |
| 49 | 39.8 | 319.3 | 0.27 | 0.0068 |
| 50 | 21.8 | 326.3 | 0.13 | 0.0058 |
| 52 | 40.7 | 328.4 | 0.36 | 0.0089 |

The spread in the values about the mean proper motion is somewhat higher than expected from the measurement errors. This is true of the entire sample, the knots in the south-western interaction zone, and also the remaining knots taken separately ($\langle\mu\rangle = 0.29 \pm 0.08$ arcsec yr$^{-1}$). It is possible that this is partly due to the fact that individual knots are moving along a line inclined to the line of sight, whereas the proper motion refers only to the projected velocity. For example, assuming the orbital inclination of the system to be 66° and an opening angle of 90° for the polar cone, one expects the knots in the polar cone to move at angles of between 21° and 111°. Since the projection factor would be the same for the radius vector and the expansion velocity, the ratio $\mu/r$ would be independent of the angle to the line of sight. The derived values of $\mu/r$ are also listed in Table 1.

The models of S89 give, after a little algebra,

$$\frac{\mu}{r} = \frac{1}{2t}\left(1 + \frac{1}{k_m}\right)$$

in the momentum-conserving case, where

$$k_m + \left(1 + \frac{2v_0 t}{\beta_m}\right)^{1/2},$$

with $v_0$ being the initial expansion velocity and $\beta_m$ being a parameter related to the ratio of the mass of the shell and the density of the ambient medium (see S89). Similarly, in the energy-conserving case we have

$$\frac{\mu}{r} = \frac{2}{3t}\left(\frac{k_e^2 + k_e + 1}{k_e^2 + k_e}\right),$$

where

$$k_e = \left(1 + \frac{3v_0 t}{2\beta_e}\right).$$

The average value of $\mu/r = 0.0095 \pm 0.0016$ yields

$$\frac{v_0}{\beta_m} = 0.012^{+0.043}_{-0.0002}\ \text{yr}^{-1}$$

in the momentum-conserving case, and

$$\frac{v_0}{\beta_e} = 0.045^{+\text{indef.}}_{-0.039}\ \text{yr}^{-1}$$

in the energy-conserving case. It should be noted here that, for significant ambient density, one expects $\mu/r > 1/2t = 0.0060$ yr$^{-1}$ in the momentum-conserving case, and $\mu/r > 2/3t = 0.0080$ yr$^{-1}$ in the energy-conserving case. Some of

the knots have values closer to or below these limits. While the measurement errors are likely to increase some of the values, it would appear that at least some knots are expanding in directions where the ambient density is low. This has the effect of increasing the upper bounds to $v_0/\beta$, more dramatically in the case of the energy-conserving case. Though more knots agree with the momentum-conserving expansion, a more detailed model based on the proper motions of a larger number of knots would be necessary for an understanding of the expansion of different regions of the shell.

The mean values derived for $v_0/\beta$ after correction for projection effects are lower than the values fitted by S89 by factors of 1.9 and 1.7 in the momentum- and energy-conserving cases, respectively. The factor increases to about 3 if one considers the polar region alone. The values of $\mu/r$ expected from the models of S89 are 0.0087 and 0.0091 $yr^{-1}$ for the momentum- and energy-conserving cases, respectively, whereas our value for the same region is $0.010 \pm 0.001$ $yr^{-1}$. Though the measured value agrees with the energy-conserving model within the observed spread, it appears likely that the mean value of $v_0/\beta$ is lower than derived by S89. The expansion velocity determined through spectroscopy at outburst was 1200 km $s^{-1}$. From an analogy with DQ Her, the velocity in the polar region could have been higher. Thus the initial expansion velocity, estimated by S89 to be 1600–1700 km $s^{-1}$, cannot be in error by a large factor. Hence one needs to increase $\beta$ by a factor of 2–3. Since $\beta$ is a measure of the ratio of the mass of the shell to the density in the circumstellar medium, this implies that either the mass of the shell is higher, or the ambient density is lower, or both.

## 3 THE OPTICAL SPECTRUM

### 3.1 Observations

Spectroscopic observations of GK Per in the 4500–7600 and 6100–9200 Å regions were made during the period 1989 November 25 to 1990 February 21 using the 102-cm telescope at VBO. Spectra were recorded at a dispersion of 5.5 Å per pixel with a resolution of ~1.8 pixel, using the Photometrics CCD system and a 250-mm camera with the UAG spectrograph at the Cassegrain focus of the telescope.

The spectrum frames were individually debiased and flat-fielded, and the one-dimensional spectra were extracted. An Fe + Ne hollow cathode source spectrum was used for wavelength calibration. At least one of the spectrophotometric standards HD 217086, HD 19445, HD 60778, Feige 15 and EG 99 were observed on each night for flux calibration. The flux-calibrated spectra were averaged to improve the signal-to-noise ratio. Spectra in the two regions were combined. The mean spectrum was corrected for interstellar reddening using $E(B-V)=0.3$ (Wu et al. 1989) and the Savage & Mathis (1979) law. All reductions were carried out using the VAX 11/780 system at VBO with the RESPECT software (Prabhu & Anupama 1991).

### 3.2 The physical conditions

Fig. 3 shows the mean, dereddened spectrum in the wavelength region 4500–9200 Å. The spectrum is a composite one, consisting of strong emission lines –H$\beta$, H$\alpha$, He I 5876, 6678, 7065 Å – over a blue continuum. He II 4686 Å and He I 7281 Å are also present. Na I D absorption is strong. The strong blue continuum and emission lines arise in the accretion disc around the white dwarf primary. Table 2 lists the emission-line fluxes, corrected for reddening. The Balmer decrement is flat, with H$\alpha$/H$\beta$ ~ 1.9, indicating high densities in the emitting medium. In the models of Drake & Ulrich (1980), such a ratio is reproduced for $T_e \gtrsim 10^4$ K, $n_e \gtrsim 10^{12}$ $cm^{-3}$ and $\tau_{Ly\alpha} \gtrsim 10^4$. The observed ratio of He I 5876/7065 = 1.9 is reproduced for $n_e \approx 10^{12}$ $cm^{-3}$, $T_e = 10^4$ K and low values of $\tau(3889)$ in the models of Almog & Netzer (1989).

Using the observed line ratios of He I 5876/H$\beta$, 5876/H$\alpha$ and He I 7065/H$\beta$, 7065/H$\alpha$, an estimate of $He^+/H^+$

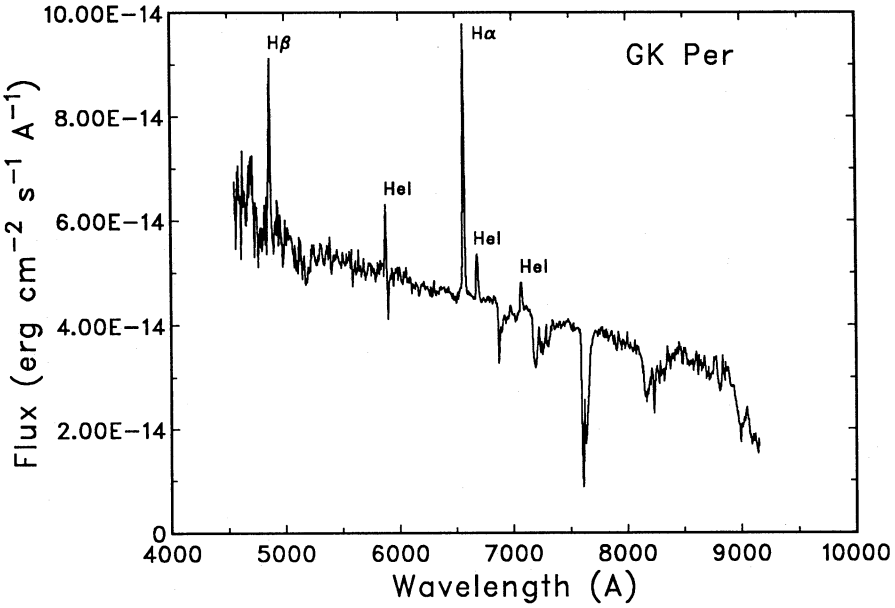


**Figure 3.** Quiescent spectrum of GK Per in the 4500–9200 Å region, corrected for $E(B-V)=0.3$. Epoch: 1989 November 25–1990 February 21.

**Table 2.** Emission-line fluxes of GK Per, corrected for $E(B-V)=0.3$.

| Line identification λ in Å | Flux $10^{-13}$ erg cm$^{-2}$ s$^{-1}$ |
|---|---|
| 4686 He II | 1.06: |
| 4861 Hβ | 2.58 |
| 5876 He I | 1.19 |
| 6563 Hα | 4.87 |
| 6678 He I | 1.00 |
| 7065 He I | 0.63 |
| 7281 He I | 0.20 |

can be made. The emissivities for the He I lines are from Almog & Netzer (1989) for $n_e=10^{12}$ cm$^{-3}$, $T_e=10^4$ K and $\tau(3889)=3.8$. Hα and Hβ emissivities from Hummer & Storey (1987) for $n_e=10^{10}$ cm$^{-3}$ are used, since hydrogen emissivities have not been calculated for $n_e>10^{10}$ cm$^{-3}$. An average value, $\langle He^+/H^+\rangle=0.20\pm0.03$, is estimated. Taking emissivities for He II 4686 Å from Hummer & Storey (1987), a value of $He^{++}/H^+=0.036$ is obtained. The derived helium abundance is $He/H=0.24\pm0.02$. In the models of Drake & Ulrich (1980), the Hβ emission measure drops steeply from $7.02\times10^{-25}$ erg cm$^3$ s$^{-1}$ at $T_e=10^4$ K, $n_e=10^{12}$ cm$^{-3}$, $\tau_{Ly\alpha}=10^4$, through $0.019\times10^{-25}$ erg cm$^3$ s$^{-1}$ at $T_e=2\times10^4$ K, $n_e=10^{12}$ cm$^{-3}$, $\tau_{Ly\alpha}=10^6$, to $0.005\times10^{-25}$ erg cm$^3$ s$^{-1}$ at $T_e=2\times10^4$ K, $n_e=10^{15}$ cm$^{-3}$, $\tau_{Ly\alpha}=10^6$. It thus appears that the above estimate of helium abundance is an upper limit. As an example, using emissivities from Drake & Ulrich (1980) for $n_e=10^{12}$ cm$^{-3}$, $T_e=1.5\times10^4$ K and $\tau_{Ly\alpha}=3.5\times10^4$, the helium abundance would be reduced to ~0.1, thus implying that the He abundance in the accreted material is close to solar. Fast novae are known to exhibit near-solar He abundance, whereas some enhancement is possible in slow novae (Boyarchuk & Antipova 1990). Since fast novae presumably contain a massive CO white dwarf, the observed He abundance is that of the matter accreted from the secondary. On the other hand, shear-mixing of accreted matter leading to an enhancement of He is expected in slow novae which contain low-mass white dwarfs which are likely to have a He core or shell. Since GK Per was a fast nova ($t_3=5$ d), we do not expect an enhancement of helium.

For $T_e=10^4$ K and $n_e=10^{10}$ cm$^{-3}$, using the observed ratio of He II 4686/Hβ, the temperature of the ionizing source is estimated to be $T_s=1.3\times10^5$ K. This estimate of temperature and the observed Hβ luminosity imply a radius $R_s\sim0.01$ $R_\odot$ for the ionizing source, assuming a covering fraction of 0.01. The temperature may be a slight overestimate and the radius an underestimate due to optical depth effects in Hβ.

### 3.3 Decomposition of the spectrum

Gallagher & Oinas (1974) estimated that the secondary contributes only 33 per cent of the total light in the blue. The total observed spectrum is thus a combination of the accretion disc spectrum and the secondary spectrum. Using standard fluxes for a K1IV star from O'Connell (1973), an estimate of the accretion disc spectrum has been made. The standard K1IV fluxes were scaled to match the observed spectrum at $\lambda\sim9000$ Å and subtracted from the observed spectrum. A suitably scaled theoretical disc spectrum of the form $f_\lambda\propto\lambda^{-7/3}$ was then fitted to the residual flux. The contributions from the individual components were estimated iteratively, such that their total matched the observed flux within 10 per cent. The best-fitting accretion disc spectrum was estimated to be $f_\lambda=10^{-5.02}\lambda^{-7/3}$ erg cm$^{-2}$ s$^{-1}$ Å$^{-1}$. Fig. 4 shows the decomposition of the observed spectrum into the secondary and accretion disc components. The dereddened continuum flux of the secondary at 5500 Å, $f_{5500}=3.4\times10^{-14}$ erg cm$^{-2}$ s$^{-1}$ Å$^{-1}$, corresponds to an absolute magnitude $M_V=+4.24$, and the estimated disc spectrum implies $M_V=+4.93$ for the accretion disc, at a

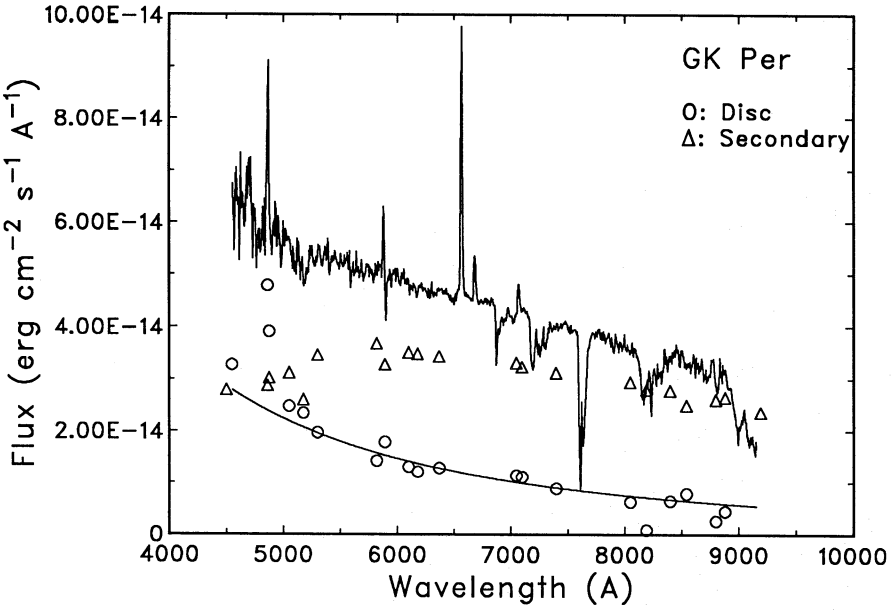


**Figure 4.** The quiescent spectrum of GK Per decomposed into the spectra of the K1IV secondary and the accretion disc.

distance of 470 pc. The secondary contributes 40 per cent of the total flux at 4400 Å.

Patterson (1991) has tried to isolate the primary photometrically, and finds that it would be too blue if the secondary were of spectral type K2IV. There is an error in the computed $B$ magnitude of the primary in Patterson's table 1 and, after correction, the $(B-V)$ colour of the primary is $-0.47$, only slightly bluer than the infinite-temperature limit. The *UBVRI* absolute magnitudes of the accretion disc, estimated from its spectrum using the transmission curves and zero-points of Bessell (1990), are +3.97, +4.94, +4.91, +4.71 and +4.61 respectively, at the assumed distance of 470 pc. Scaling the *UBVR* absolute magnitudes of the total system given by Patterson to this distance, and assuming the K2IV stellar magnitudes adopted by him, one can fit the relation (using the SIXLIN program of Isobe et al. 1990)

$$\frac{\text{total light}}{\text{secondary}} = (0.808 \pm 0.015) + (0.842 \pm 0.003) \times \frac{\text{accretion disc}}{\text{secondary}},$$

with a correlation coefficient of better than 0.9999 and a standard error of 0.5 per cent. This implies that the accretion disc is 16 per cent fainter than estimated here and the secondary 19 per cent (0.23 mag) fainter than assumed by Patterson. The $I$ magnitude has not been used in the fit, since it is ~0.5 mag fainter than expected from the above relation (see further discussion below). The implied value of $M_V$ is 3.99 mag for the secondary. With these estimates, the secondary contributes 51 per cent of the total light in the blue.

Comparing the estimate of $M_V = +4.9$ for the accretion disc with the theoretical relationship of Webbink et al. (1987), one can estimate the mass transfer rate to be $\dot{M} = 3.5 \times 10^{-9}$ $M_\odot$ yr$^{-1}$ $= 2.4 \times 10^{17}$ g s$^{-1}$ for a 0.9-$M_\odot$ white dwarf and an inclination angle of 66°. An increase in the inclination results in an increase in the estimate of mass transfer rate. This value is higher than the value suggested by the models of Kim et al. (1992) for quiescence, but well below their deduced mass transfer rates during outburst. It should be noted that the epoch of the present observations is only a few months later than the peak of the 1989 outburst.

The ultraviolet–optical spectrum of the disc in GK Per is found to have a maximum at 3000 Å (Wu et al. 1989). The flux deficit shortward of this wavelength has been ascribed to the disruption of the inner part of the accretion disc as a result of the magnetic field of the white dwarf. Bianchini & Sabbadin (1983) obtained an estimate of the disc inner radius of $r_{in} = 1.2 \times 10^9$ cm. The $I$ magnitudes during 1983 October and 1991 January (Patterson 1991) were lower than expected from the 'accretion disc + secondary' model derived here. Assuming that the deficit at $I$ is real, one can estimate that the outer radius of the disc is $r_{out} \simeq 3 \times 10^{10}$ cm, using the standard temperature profile of a steady accretion disc (Webbink et al. 1987). This value is smaller than the circularization radius ($> 10^{11}$ cm) for the period of 1.997 d (King 1989). The estimates of disc radius during the outburst, however, are of the order of the circularization radius (Bianchini, Sabbadin & Hamzaoglu 1982). We thus conclude that the disc is smaller at quiescence than during outburst, which agrees with the idea that the outbursts are triggered by an increase in the mass transfer rate. It is significant in this context that GK Per was 1 mag brighter than usual at $I$ a few months before the 1986 outburst (Patterson 1991).

## 4 CONCLUSIONS

The shell of GK Per is clumpy and asymmetric. In [N II] it is flattened in the south-western and north-eastern directions, where its interaction with the circumstellar medium is most obvious. The knots in [N II] and [O III] generally coincide in all regions except in the radio ridge region. This difference has been attributed to spatial variations in the physical conditions of the knots (Seitter & Duerbeck 1987; S89). A comparison of the published [O II] images (S89) shows that there is an enhancement of [O II] and [O III] along position angles 130° and 300°, indicating a possible enhancement of oxygen over nitrogen along the equatorial torus. A combination of [O III] and [O II] images shows a symmetric distribution of oxygen in the shell, whereas [N II] is weak or absent in the equatorial region.

Proper motion measurements of the knots in [N II] give a mean expansion rate of $0.31 \pm 0.07$ arcsec yr$^{-1}$ ($690 \pm 150$ km s$^{-1}$ at a distance of 470 pc). This value is consistent with the momentum- and energy-conserving expansion models developed by S89. A correction for projection effects, however, implies that the ratio of shell mass to circumstellar density as derived by S89 requires an upward revision by a factor of 2–3. It seems possible that a combination of proper motion and radius information will yield more complete information on the kinematics of the shell.

The optical spectrum of GK Per is composite, consisting of hydrogen and helium emission lines superposed on the absorption spectrum from the secondary. The emission lines arise in the accretion disc around the white dwarf primary. The H$\alpha$/H$\beta$ ratio of ~1.9 and also the observed He I line ratios indicate high densities of $\sim 10^{12}$ cm$^{-3}$ and $T_e \geq 10^4$ K. Using the He II 4686/H$\beta$ line ratio, a temperature of $1.3 \times 10^5$ K is obtained for the source ionizing the accretion disc. The observed H$\beta$ luminosity, together with this estimate of temperature, implies a white dwarf of radius 0.01 $R_\odot$. The helium abundance in the accretion disc is probably close to solar. The flux from the accretion disc is $f_\lambda = 10^{-5.02} \lambda^{-7/3}$ erg cm$^{-2}$ s$^{-1}$ Å$^{-1}$. The corresponding $M_V = +4.93$ at a distance of 470 pc implies a mass transfer rate of $\dot{M} = 3.5 \times 10^{-9}$ $M_\odot$ yr$^{-1}$. The accretion disc spectrum probably turns over in the $I$ band, indicating an outer radius $r_{out} = 3 \times 10^{10}$ cm during quiescence. The presence of a magnetic field is likely to affect the above estimates. Bianchini & Sabbadin (1983) found that the inner regions of magnetic discs are cooler and the outer regions hotter compared to non-magnetic discs. Inclusion of this effect would decrease the estimate of mass transfer rate and increase the estimate of outer radius. If the scatter seen in the $I$ magnitudes of Patterson (1991) is real, then monitoring of GK Per in this band may yield information on the evolution of the accretion disc radius with time.

## ACKNOWLEDGMENTS

This work forms a part of the PhD thesis of GCA, submitted to the Bangalore University. She thanks the Director, IIA, for

all the facilities provided. The paper has benefited greatly from the comments of M. F. Bode and H. W. Duerbeck. We also thank H. W. Duerbeck for making the 1984 Calar Alto image of GK Per available to us.

## REFERENCES

Almog Y., Netzer H., 1989, MNRAS, 238, 57
Bessell M., 1990, PASP, 102, 1181
Bianchini A., 1990, AJ, 99, 1941
Bianchini A., Sabbadin F., 1983, A&A, 54, 393
Bianchini A., Hamzaoglu E., Sabbadin F., 1981, A&A, 99, 392
Bianchini A., Sabbadin F., Hamzaoglu E., 1982, A&A, 106, 176
Bianchini A., Sabbadin F., Favero G. C., Dalmeri I., 1986, A&A, 160, 367
Bode M. F., Seaquist E. R., Frail D. A., Roberts J. A., Whittet D. C. B., Evans A., Albinson J. S., 1987, Nat, 329, 519
Boyarchuk A. A., Antipova L. I., 1990, in Cassatella A., Viotti R., eds, Physics of Classical Novae. Springer-Verlag, Berlin, p. 97
Cannizzo J. K., Kenyon S. J., 1986, ApJ, 309, L43
Couderc P., 1939, Ann. Astrophys., 300, 788
Crampton D., Cowley A. P., Fisher W. A., 1986, ApJ, 300, 788
Curtis H. N., 1919, Lick Obs. Bull., 10, 35
Drake S. A., Ulrich R. K., 1980, ApJS, 42, 351
Duerbeck H. W., 1987, Ap&SS, 131, 461
Gallagher J. S., Oinas V., 1974, PASP, 86, 952
Hessman F. V., 1989, MNRAS, 239, 759
Hummer D. G., Storey P. J., 1987, MNRAS, 224, 801
Hurst G. M., 1989, IAU Circ. 4819
Isobe T., Feigelson E. D., Akritas M. G., Babu G. J., 1990, ApJ, 364, 104
Kim S.-W., Wheeler J. C., Mineshige S., 1992, ApJ, 384, 269
King A. R., 1989, in Bode M. F., Evans A., eds, Classical Novae. John Wiley, Chichester, p. 17
Kraft R. P., 1964, ApJ, 139, 457
Norton A. J., Watson M. G., King A. R., 1988, MNRAS, 231, 783
O'Connell R. W., 1973, AJ, 78, 1074
Patterson J., 1991, PASP, 103, 1149
Payne-Gaposchkin C., 1957, The Galactic Novae. North Holland, Amsterdam
Pease F. G., 1917, PASP, 29, 256
Perrine C. D., 1902, ApJ, 16, 249
Prabhu T. P., Anupama G. C., 1991, Bull. Astron. Soc. India, 19, 97
Reynolds S. P., Chevalier R. A., 1984, ApJ, 281, L33
Ritchey G. W., 1901, ApJ, 14, 167
Savage B. D., Mathis J. S., 1979, ARA&A, 17, 73
Schaefer B., 1988, ApJ, 327, 347
Seaquist E. R., Bode M. F., Frail D. A., Roberts J. A., Evans A., Albinson J. S., 1989, ApJ, 344, 805 (S89)
Seitter W. C., Duerbeck H. W., 1987, in Bode M. F., ed., RS Ophiuchi (1985) and the Recurrent Nova Phenomenon. VNU Sci. Press, Utrecht, p. 71
Swope H., 1940, Harvard Bull. No. 913, 11
Vogt N., 1989, in Bode M. F., Evans A., eds, Classical Novae. John Wiley, Chichester, p. 225
Watson M. G., King A. R., Osborne J., 1985, MNRAS, 212, 917
Webbink R. F., Livio M., Truran J. W., Orio M., 1987, ApJ, 314, 653
Wu C.-C., Panek R. J., Holm A. W., Raymond J. C., Hartmann L. W., Swank J. H., 1989, ApJ, 339, 441